Citation: Pema, T. Aoki (2020), Seismic evaluation and retrofitting of traditional Bhutanese stone masonry residential house, Synopsis of IISEE-GRIPS master report.

SEISMIC EVALUATION AND RETROFITTING OF TRADITIONAL BHUTANESE STONE MASONRY RESIDENTIAL HOUSE

PEMA[1,2] **Supervisor: Takayoshi AOKI[3]**

ABSTRACT

Traditional houses form an integral part of the unique landscape of Bhutan. Unfortunately, these structures are highly vulnerable to seismic activities, but there are only limited research works in this field. Thus this paper deals explicitly on the development of seismic technology for strengthening such random rubble masonry structures in mud and cement mortars. This study's basis is the full-scale quasi-static test conducted on two-storied residential houses designed based on a representative sampling of traditional houses for unreinforced and retrofitted types. The proposed seismic intervention is the mesh-wrap retrofitting technique. Furthermore, we developed a numerical model based on the Finite Element Method and conducted non-linear pushover analyses, which was capable of simulating the experiment. Finally, this study presents the first-of-its-kind conventional fragility curves for traditional Bhutanese residential houses, generated based on the Capacity Spectrum Method.

Keywords: Stone masonry, Retrofitting, Experimental works, Finite Element Method, Fragility curves.

1. INTRODUCTION

The masonry is the earliest and oldest form of construction material in the history of humanity. Today, stone masonry is still one of Bhutan's indigenous construction practices, which constitutes of historical monuments to a simple traditional house. Over the past decade, Bhutan has witnessed seismic events (of a magnitude not exceeding M7). Such seismic events have manifested into the damage of traditional houses (load-bearing structures), thus raising critical concerns about its structural integrity and seismic capacity. On the other hand, there is a rich repository of traditional knowledge systems in Bhutanese indigenous construction materials, techniques and methods. Therefore, it is important to evaluate its seismic performance through an engineered lens considering its relevance to the social and economic aspects of the rural community residing in such seismic prone areas. This study focuses on clarifying the seismic performance of such traditional stone masonry structures and proposes seismic retrofitting measures, i.e., mesh-wrap retrofitting technique. It confirms the efficacy of the proposed method, both experimentally and numerically.

2. EXPERIMENTAL PROGRAM

2.1. Test specimen

The test specimen was designed based on the representative sampling of all architectural forms of Bhutanese house. The technique for weaving the stone and construction of walls follows the current trend of construction practice. The specimen has a floor area of 8.1m x 5.4m and a floor height of 3.15m and 3.75m for the first and second floors, respectively (Figure 1). The thickness of the wall was 600mm throughout the wall height. The characteristic feature of floor plans found in Bhutanese house resulted in differential wall distribution in the consequent floors due to the large opening of the front façade on

[1] Department of Culture, Ministry of Home and Cultural Affairs, Bhutan.
[2] IISEE-GRIPS master course student.
[3] Professor, Nagoya City University, Japan.

the second floor. We constructed two structures following this design only to be different by binding mortar, i.e., in mud mortar (USMM) and cement mortar (USMC).

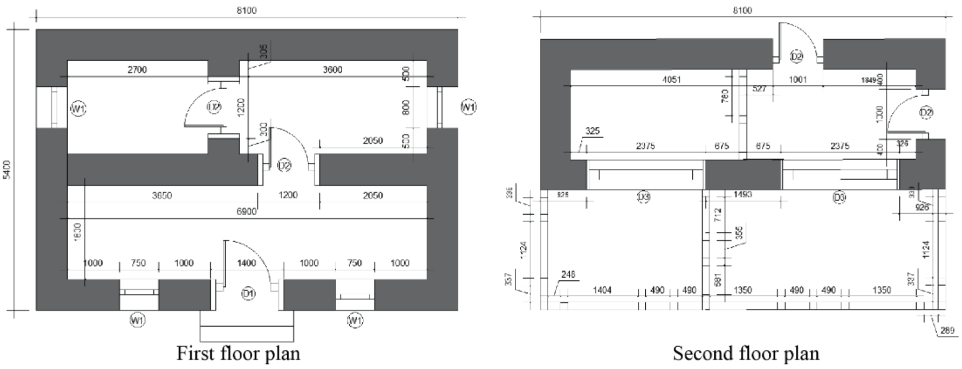

Figure 1. Plan of the target specimen.

2.2. Retrofitting measure

For the community to accept the proposed technique and achieve widespread utilization of the proposed retrofitting methods, it is essential to ensure that the materials are readily available. The processes need to be practical, pragmatic, and user-friendly. It is also crucial to consider the economic viability, and it does not obstruct the community's social perception. Considering all the reasons mentioned above, we decided to design, check on the feasibility and structural performance of the proposed mesh-wrap techniques at a smaller scale, and then gradually adopted the same to full-scale specimens. Two types of mesh with different sizes of 12 gauge/ 1.83mm with 34x34mm^2 openings (primary mesh) and 16 gauge/ 1.45mm with 28x28mm^2 openings (secondary mesh) were selected. The primary mesh was fixed to the stone masonry substrate, both externally and internally. For the limitation of the sizes, the primary mesh overlapping was unavoidable for both vertical and horizontal directions. It required further intervention for continuity and eradication of the creation of a weak joint, thereby secondary meshes were necessary. The requirement of minimum overlap is 300mm. This series of work encapsulates the background idea for the retrofitting technique: Fixing of primary mesh, overlapping at corners and joints, application of two coats of cement plaster- 30mm thick finished surface and provide timber bracings at floor diaphragm (Figure 2). The retrofitted counterpart of the USMM and USMC specimens are hereafter referred to as RSMM and RSMC.

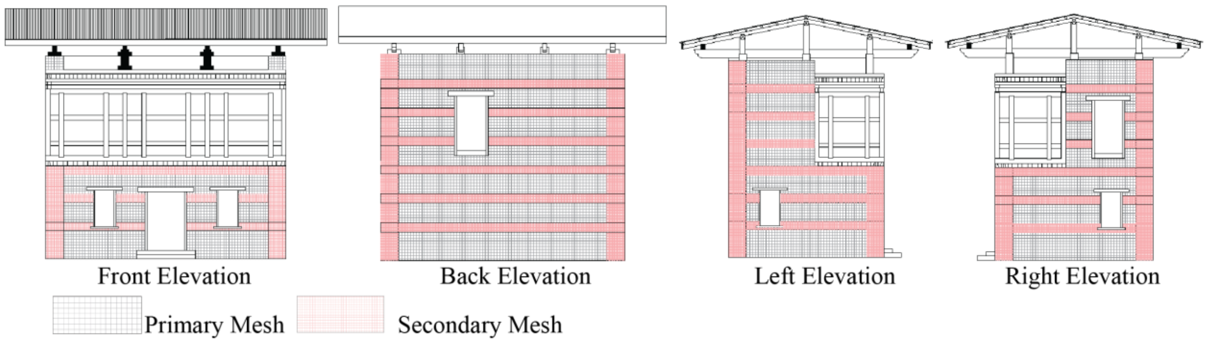

Figure 2. Design of mesh-wrap technique applied to the full-scale specimen.

2.3. Test-set up and capacity curves

The quasi-static test setup utilizes two 1000kN and two 500kN capacity static jacks, positioned at first and second floors. There are two types of displacement transducers: ten laser transducers and four linear variable displacement transducers (LVDTs) at three levels of the test specimen placed at the loading and the free side. We used a multi-channel dynamic strain-meter DS-50A for data logging with the LAN interface setting, and the data sampling rate was 100 Hz. The monotonic static lateral loads applied to the specimen was the displacement-controlled loading with manual synchronization of the hydraulic pumps (Figures 3-a and 3-b). The load transfer mechanism involves using a built-up H-section from the static jack to the specimen, to achieve uniform load application throughout the point of application.

(a) (b) (c)

Figure 3. (a) Schematic full-scale quasi-static test setup, (b) Real scenario experimentation setup and (c) FE-numerical model with loading constraints.

The specimen was subjected to one-half cycles of displacement-controlled loading (monotonic static lateral force) for each specified drift target value. The USMC specimen was tested for a drift of 1/1000 (0.01%), 1/750 (0.13%), 1/400 (0.25%) up to 1/300 (0.33%) and the RSMC specimen was further subjected to a drift of 1/750 (0.13%), 1/500 (0.2%), 1/250 (0.4%), 1/150 (0.67%), 1/100 (1%), 1/75 (1.33%) and 1/50 (2%). The RSMM specimen was subjected to a drift of 1/2000 (0.05%), 1/1000 (0.1%), 1/750 (0.13%), 1/500 (0.2%), 1/250 (0.4%), 1/150 (0.67%), 1/100 (1%), 1/90 (1.11%) and 1/80 (1.25%). Here, the storey-drift is the ratio of the lateral displacement to the floor height. The peak base shear recorded for USMC was 765 kN, and that for RSMC and RSMM was 1200 kN and 783 kN, respectively (Figure 4-a). An increment in the base shear capacity of 56.6% was achieved with the adopted mesh-wrap retrofitting in the stone masonry house in cement mortar. Here, the base shear is the summation of the storey shears at first and roof floors.

3. FINITE ELEMENT ANALYSIS

The numerical simulation is made in a finite element program DIANA 10.4. DIANA offers many constitutive material models depending on the nature of the analysis, and here we use the total strain rotating crack model. The basis for selecting this constitutive model is a cautious compromise between the accuracy of the results and computation time. After selecting the non-linear material model, we need to define the stress-strain relationships for different types of behavior clearly. The adopted hysteretic behavior takes into account the exponential tension-softening for the tensile behavior and parabolic hardening with subsequent softening for the compressive behavior, which is considered only for the masonry (Angelillo et al., 2014). In this model, the shear behavior is adequately captured and updated as the damage progression happens. The FE simulation follows the macro-modeling approach for the full-scale house.

The numerical FE-model has 9070 numbers of finite elements. The structural walls of this FE model consist of 3492 numbers of an eight-node isoparametric solid brick element (HX24L), which constitutes of non-linear property. The rest of the material has only linear material properties considered. The adopted mesh size for all the FE elements is 300mm. In this pushover analysis, the target structure's non-linear behavior was evaluated by applying lateral loads in user-controlled successive load steps. A multi-point tying option available in DIANA, i.e., connecting all the slave nodes (yellow dot circles) to the master mode (red dot circle) as shown in Figure 3-c, was used to simulate the actual loading condition of the experiment. The iterative process for solving the system of equations follows the Newton-Raphson method and convergence criteria set in the form of energy, displacement, and forces. A line search algorithm was also adopted for the improvement of the convergence. Table 1 summarizes the material properties adopted for FE numerical simulation for the full-scale tests. The mesh-wrap components' properties follow the material characterization tests of the uniaxial compression test of the cement mortar and tension coupon test of mesh composite. The FE-numerical model was in good agreement with the experimental campaign. The capacity curve of the FE-model for RSMC response simulated well in the linear elastic region where the capacity curves are parallel to each other, which then diverged in the non-linear region.

The peak load of FE numerical analysis is 845.70kN. The recorded peak load from the experiment is 765kN, but this is not the ultimate load since we stopped the investigation at a drift of 1/300 (0.33%) for retrofitting purposes (RSMC). At 0.2% storey drift, the corresponding base shear is 716.25kN and 736.30kN for the experiment and FE model, respectively (Figure 4-b). The capacity curve with a 50% reduction of the tensile property of mesh composite, indicated by the black dotted curve "FE-RSMC-50%" and "FE-RSMM-50%, is the best-fit capacity curve (Figures 4-c and 4-d). The base shear for USMM from the FE analysis is 438.38kN.

Table 1. Adopted material and physical properties for full-scale specimen numerical FE simulations.

Material Properties	Specimen with mud mortar	Specimen with cement mortar
Mass density, ρ (kg/m^3)	2300	2300
Elastic Modulus, E (MPa)	150	350
Poisson's ratio, υ	0.20	0.20
Compressive strength, f_c (MPa)	0.60	3.00
Compressive fracture energy, G_{fc} (N/mm)	0.96	4.80
Tensile strength, f_t (MPa)	0.02	0.15
Tensile fracture energy, G_f^I (N/mm)	0.0016	0.012

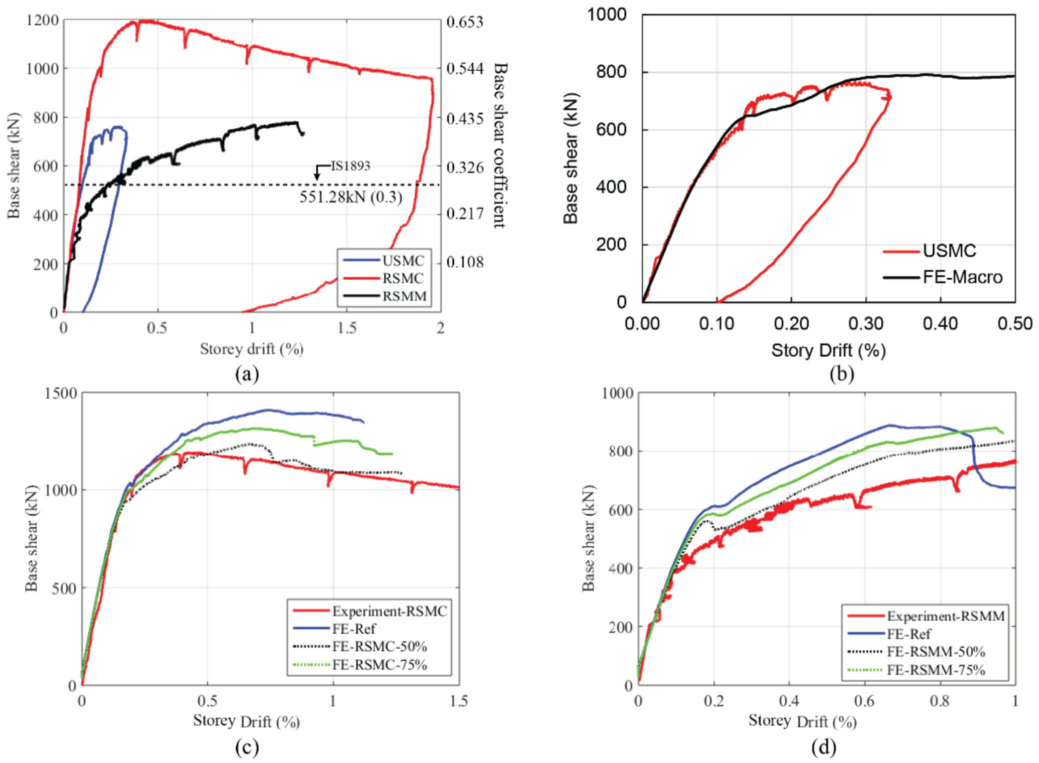

Figure 4. (a) Experimental capacity curves; Comparison of FE generated capacity curve to experimentally obtained capacity curve for (b) USMC (c) RSMC and (d) RSMM.

4. VULNERABILITY ASSESSMENT

The concept of a vulnerability assessment is related to Probabilistic Safety Assessment (PSA) and fragility assessment. A fragility curve is a statistical tool that utilizes the results obtained from an appropriate structural response assessment. It is capable of presenting complex engineering results in graphical formats for general-purpose. Here, the seismic performance assessment utilizes the Capacity Spectrum Method (CSM). The CSM is a simplified non-linear static analysis procedure, and nowadays, extensively used to explain the structural performance of a structure. Freeman et al. (1975) first proposed the CSM method, and it was subsequently included in ATC-40. It has also become a subject of study in the last two decades. In Japan, the seismic design requirement in the Building Standard Law of Japan (BSLJ) was made inclusive of a performance-based design framework in June 2000 (Otani et al., 2000). In this study, the CSM analysis follows the procedure specified by the BSLJ. For the CSM method, it is necessary to convert the capacity curve, generally expressed in terms of base shear and roof displacement, to a capacity spectrum. Capacity spectrum is the representation of the capacity curve in the Acceleration-Displacement Response Spectra (ADRS) format (i.e., Spectral acceleration S_A versus Spectral Displacement S_D), after Mahaney et al. (1993). The pushover analysis (using Finite Element solutions) with external force distribution proportional to the first mode, provides the S_A - S_D curve (Capacity spectrum) typically. Here, the author has an advantage with the availability of experimental pushover curves based on a full-scale quasi-static test of building prototype.

Every country's seismic code presents a traditional response spectra S_A versus T (Time period) for building design purposes. This response spectrum also requires the conversion in the ADRS format. In addition to the conventional response spectra obtained from building codes and standards, we have selected appropriate ground motion records for the structural response assessment. We chose cautiously seven (7) earthquake ground motions (Figure 5-right), exclusive of response spectra of IS 1893, and NBC-105. All input demand spectrums were scaled appropriately to different levels as per the capacity of the structures. The intersection of the capacity curve and the demand spectrum for an appropriate equivalent damping ratio is called Performance point (Figure 5-left). We get a single performance point for one PGA level of the particular EQ spectrum, thus obtaining multiple performance points for USMC, RSMC and RSMM structures, for a suite of EQ earthquake response spectra, which forms the basis for the generation of fragility curves.

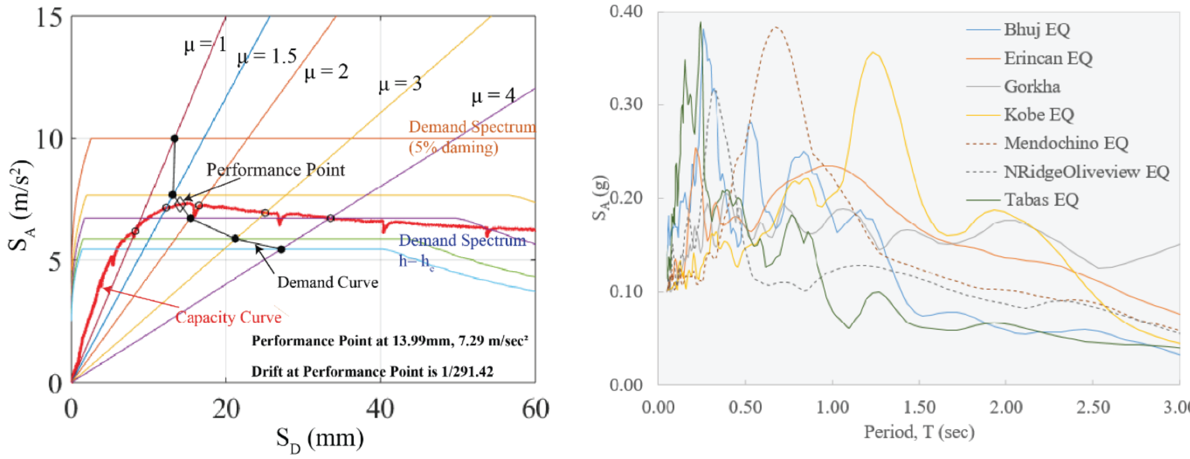

Figure 5. Performance point for PGA of 0.4g of IS 1893-2016 for RSMC house using the CSM method (Left) and Acceleration response spectra for the selected earthquake records at 5% damping (Right).

The fragility curve expresses the probability that the target structure will exceed a specific damage state as a function of earthquake intensity parameters (such as PGA, PGV, SA, etc.). In this study, the author uses the methodology proposed by Wen et al. (2004) for the generation of fragility curves. The probability that the given structure exceeds the limit-damage state for given ground motion intensity is given by Eq. (1).

$$(LS_i/GMI) = 1 - \phi\left(\frac{\lambda_{CL}^{i} - \lambda_{D/GMI}}{\beta_{D/GMI}}\right) \quad (1)$$

where $P(LS_i/GMI)$ is the probability of exceeding a particular limit state given ground motion intensity (GMI), ϕ (•) is the standard normal cumulative distribution function, λ_{CL}^{i} is ln (median storey drift for a particular limit state, i), $\lambda_{D/GMI}$ is ln (calculated median demand storey drift given the GMI from the best fit power-law line) and $\beta_{D/GMI}$ is the demand uncertainty. The two parameters $\lambda_{D/GMI}$ and $\beta_{D/GMI}$ are given by Eqs. (2) and (3):

$$\lambda_{D/GMI} = Ina_1 + a_2 \ln(GMI) \quad (2)$$

$$\beta_{D/GMI} = \sqrt{\frac{\sum_{k=1}^{n}\left[LN(GMI_k) - \lambda_{D/GMI}(GMI_k)\right]^2}{n-2}} \tag{3}$$

The constants a_1 and a_2 are obtained through linear regression analysis, by plotting natural logarithmic values corresponding to storey drift and PGA (which is the GMI). Following the statistical analysis, three fragility curves are generated (Figure 6) for USMC, RSMC and RSMM, a plot showing the probability of exceeding the damage limit-state threshold values as a function of ground motion intensity (PGA). Three categories of damage limit states, i.e., Immediate Occupancy (IO), Life Safety (LS), and Collapse Prevention (CP), is defined based on the observation of the full-scale quasi-static test.

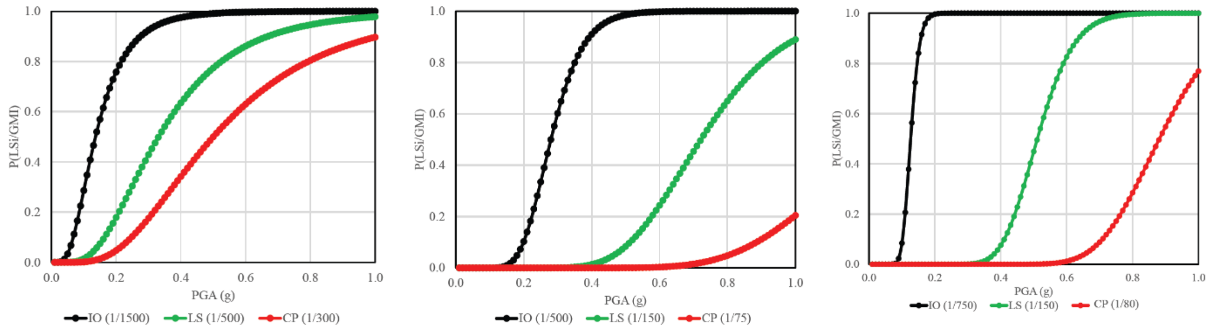

(a) USMC (b) RSMC (c) RSMM

Figure 6. Fragility curves for traditional Bhutanese residential houses.

5. CONCLUSION

The need for more experimental studies to clarify traditional structures and materials' behavior is of paramount importance. This study is one such effort to preserve and promote traditional structures. The full-scale quasi-static test shows that the proposed mesh-wrap retrofitting technique effectively increases the seismic capacity of such structures, i.e., 1.58 times the base shear of conventional (unreinforced) structures. The study shows that there is a need to increase the seismic capacity of stone masonry in mud mortar, and more scientific studies are required. Finally, the first of its kind conventional fragility curves are developed based on experimental capacity curves for traditional Bhutanese houses.

ACKNOWLEDGEMENTS

This research was conducted during the individual study period of the training course "Seismology, Earthquake Engineering and Tsunami Disaster Mitigation" by the Building Research Institute, JICA, and GRIPS. I want to express my sincere gratitude to my supervisor Prof. Takayoshi Aoki and co-supervisor Asst. Prof. Kshitij Charana Shrestha of Nagoya City University, for their valuable advice and thoughtful guidance. I will always remain grateful to Dr. Tatsuya Azuhata, Director and Dr. Mai Ito of the International Institute of Seismology and Earthquake Engineering (IISEE), who are my advisors. I would also like to express my sincere gratitude to the National Graduate Institute for Policy Studies (GRIPS) and Japan International Cooperation Agency (JICA) for providing me with this opportunity to undertake the integrated master's program. I want to thank the Royal Government of Bhutan and, in particular, the Department of Culture under the Ministry of Home and Cultural Affairs for allowing me to pursue further studies.

REFERENCES

Angelillo, M., Lourenço, P. B., and Milani, G. (2014). In *CISM International Centre for Mechanical Sciences, Courses and Lectures*.

Freeman, S. A., Nicoletti, J. P., and Tyrrell, J. B. (1975), *Proceedings of US National Conference on Earthquake Engineering*, 113–122.

Mahaney, J. A., Paret, T. F., Kehoe, B. E., and Freeman, S. A. (1993). *National Earthquake Conference*.

Otani, S., Hiraishi, H., Midorikawa, M., and Tashigawara, M. (2000). *ACI Special Publication*, *197*, 87–104.

Wen, Y. K., Ellingwood, B. R., and Bracci, J. (2004). *Mid-America Earthquake Center Project*, 1–101.